Preparation of wrapped carbon nanotubes poly(4-vinylpyridine)/MTO based heterogeneous catalysts for the oxidative desulfurization (ODS) of model and synthetic diesel fuel

Davide Piccinino [a], Issam Abdalghani [b], Giorgia Botta [a], Marcello Crucianelli [b,*], Maurizio Passacantando [b], Maria Laura Di Vacri [c], Raffaele Saladino [a,*]

[a] Department of Biological and Ecological Sciences, University of Tuscia, Via S. Camillo de Lellis snc, I-01100 Viterbo, Italy
[b] Department of Physical and Chemical Sciences, University of L'Aquila, Via Vetoio, I-67100 Coppito (AQ), Italy
[c] Gran Sasso National Laboratories, INFN, S.S. 17/bis km 18 + 910, I-67010 Assergi (AQ), Italy

ABSTRACT

The preparation of novel wrapped carbon nanotubes poly(4-vinylpyridine)/methyl trioxorhenium based heterogeneous catalysts has been reported by two different procedures: a) the wrapping by grinding of multiwall carbon nanotubes with pre-formed adducts, respectively, [poly(4-vinylpyridine)·methyltrioxorhenium] or [poly(4-vinylpyridine)-N-oxide·methyltrioxorhenium] and, b) the loading of methyltrioxorhenium on previously wrapped multiwall carbon nanotubes with poly(4-vinylpyridine) and poly(4-vinylpyridine)-N-oxide resins. The novel catalysts were characterized by SEM, TEM, ICP-MS and XPS analyses. Both types of catalysts were efficient systems in the oxidation of recalcitrant aromatic sulfur derivatives with H_2O_2, as representative models of oxidative desulfurization processes, affording the corresponding sulfones with yields ranging from moderate to quantitative. The oxidation of a complex model fuel oil and of synthetic diesel fuel, under optimal experimental conditions, is also reported. The performance of novel catalysts was dependent on the specific procedure applied for the immobilization of the active species, and was more efficient for both model oil and synthetic diesel fuel samples (with quantitative conversions and selectivities to the corresponding sulfones), than for isolated substrates.

1. Introduction

The removal of sulfur compounds in fuel is an important tool for the environmental protection [1], since the combustion process produces SO_x derivatives that affect the stability of the atmospheric ozone layer, increasing the formation of acid rains [2]. Therefore, the sulfur content in diesel fuel is limited by U.S. Environmental Protection Agency (EPA) and Euro V standard protocols [3]. Hydrodesulfurization (HDS) is the conventional procedure for the removal of sulfur derivatives in fuel [4] by hydrogenolysis at both high temperature (300–400 °C) and pressure (10–130 atm) [5]. However, HDS achieves limited performances in the removal of recalcitrant aromatic compounds, such as benzothiophene (BT), dibenzothiophene (DBT) and their derivatives, which can irreversibly inactivate the catalyst, influencing the kinetic and the performance of the reactors [6]. The oxidative desulfurization (ODS) is a promising alternative to HDS [7]. In the ODS process, BT and DBT derivatives are oxidized to corresponding sulfones and sulfoxides under low temperature and pressure conditions, followed by extraction or adsorption processes with polar phases [8]. The oxidation of BT and DBT derivatives in the ODS process is usually performed by stoichiometric oxidants, such as sodium bromate ($NaBrO_3$) [9], potassium permanganate ($KMnO_4$) [10], carboxylic and sulfonic peracids [11], nitric acid (HNO_3), tert-butyl-hydroperoxide (TBHP) [12], superoxides [13] and ozone [14]. Among the stoichiometric reagents, hydrogen peroxide (H_2O_2) is frequently applied due to its environmental benign properties [15]. In a previous study, we described the activation of H_2O_2 in the oxidation of BT and DBT derivatives with poly(4-vinylpyridine)/methyltrioxorhenium (CH_3ReO_3, MTO) adducts as heterogeneous catalysts [16]. In these reactions, MTO forms mono-peroxorhenium [$MeRe(O)_2(O_2)$] and bis-peroxorhenium [$MeRe(O)(O_2)_2$] complexes [17], which can

transfer the oxygen atom to sulfur substrates [18]. The heterogeneous catalysis is of relevance in ODS processes, since it reduces the leaching of active species and favors the recovery and reuse of the catalyst for successive transformations [19]. In the last years, multiwall carbon nanotubes (CNTs) have been used to design novel and efficient nanostructured heterogeneous catalysts [20]. CNTs are quasi one-dimensional materials (lengths range from less than 100 nm to several centimetres, and diameters of typically 0.8–2 nm and 5–20 nm), and show unique electronic, mechanical and structural properties [21]. They are chemically stable with high surface to volume ratio, and undergo chemical functionalization for the preparation of catalysts with specific and carefully tuned properties. The combination of CNTs with titanium species [22], polyhetero acids (Cs2·5H0·5PW$_{12}$O$_{40}$) [23], manganese oxides [24], and palladium derivatives [25], has been reported in ODS model processes, with different degree of success depending on the specific experimental conditions. Recently, we described the use of CNTs as anchoring supports for different oxidative enzymes [26]. Here, we describe the preparation of a novel family of MTO heterogeneous catalysts based on either, the immobilization of preformed poly(vinyl-4-pyridine)·MTO [PVP·MTO] or poly(vinyl-4-pyridine-N-oxide)·MTO [PVPNO·MTO] adducts on pristine CNTs, or the direct loading of MTO on previously wrapped CNTs with PVP and PVPNO resins. The novel catalysts were successfully used for the activation of H$_2$O$_2$ in the oxidation of BT and DBT derivatives, and in the treatment of model fuel oil (MF) and synthetic diesel fuel (SDF) as representative systems for the ODS process.

2. Experimental

2.1. Materials and equipments

Methyltrioxorhenium (MTO), H$_2$O$_2$ (35% w/w, aqueous solution), poly(4-vinyl pyridine) PVP-2% cross-linked with divinylbenzene, 3-methyl-thiophene (3-MeT), 2-methyl-benzothiophene (2MeBT), 3-methyl-benzothiophene (3MeBT), dibenzothiophene (DBT), 4,6-dimethyl-dibenzothiophene (DMDBT), and CNTs (D = 110–170 nm; L = 5–9 μm) were obtained from a commercial source (Aldrich). All commercial products and solvents (CH$_2$Cl$_2$, n-octane, CH$_3$CN) were of the highest grade available. The diesel fuel sample was obtained from a commercial italian source, having a density of 0.713 g/mL, 0.34% w/w of total sulfur, 73 ppm of total nitrogen (N), and 18% w/w of total aromatic fractions. The reaction mixtures were analyzed by a Hewlett Packard 6890 series gas chromatograph equipped with a FID, using a 30 m × 0.32 mm × 0.25 mm film thickness (cross-linked 5% phenylmethylsiloxane) column, and helium as carrier gas. The identification of the peaks by gas-chromatography mass-spectrometry (GC–MS) has been performed by means of a Varian 2000 GC–MS instrument. Yields and conversions have been quantified using n-hexadecane as internal standard or, when necessary, after flash-chromatographic purification (silica gel, 230–400 mesh). Product yields were calculated on the basis of the substrate conversion. ^{1}H and ^{13}C NMR spectra were recorded on a Bruker AC 400 MHz spectrometer. Inductively coupled plasma mass spectrometry (ICP-MS) analyses were performed on Agilent 7500a model ICP mass spectrometer.

2.2. Catalyst preparation

2.2.1. Preparation of catalyst CNT/MTO I

CNTs (10 mg) were suspended in EtOAc (10 mL) and treated in ultrasonicator apparatus for 30 min. MTO was added to the suspension of CNTs in EtOAc (1:1, 1:2 and 1:5 CNT/MTO w/w ratio) at 25 °C for different times (30, 60, and 2 h) under magnetic stirring. At the end, the catalyst CNT/MTO I was recovered by centrifuga-

tion (12.000 rpm), washed with a low amount of EtOAc (2.0 mL) and dried. The washing solvent was stored in order to evaluate the loading factor (LF). The highest LF was obtained for CNT/MTO 1:2 w/w ratio, after 2 h.

2.2.2. Preparation of catalysts CNT/[PVP·MTO] II and CNT/[PVPNO·MTO] III

The PVP·MTO and PVPNO·MTO adducts were prepared as previously reported [16]. Briefly, the appropriate resin (80 mg) was suspended in EtOH (2 mL), and treated with freshly prepared MTO (20 mg, 0.08 mmol) under magnetic stirring for 1 h at 25 °C. At the end, the mixture was filtered and washed with EtOH (2.0 mL) to yield the desired adducts. The wrapping of preformed PVP·MTO and PVPNO·MTO adducts on CNTs was performed by grinding the mixture in agate mortar (CNT/adduct 1:3 w/w) for 20 min at 25 °C. At the end, the material was suspended in EtOAc (5.0 mL) and catalysts CNT/[PVP·MTO] II and CNT/[PVPNO·MTO] III were recovered by centrifugation (12.000 rpm), washed with a low amount of EtOAc (2.0 mL) and dried. The washing solvent was stored in order to evaluate the LF.

2.2.3. Preparation of catalysts [CNT/PVP]/MTO IV and [CNT/PVPNO]/MTO V

The wrapping by grinding of CNTs with poly(4-vinyl pyridine) [CNT/PVP] or poly(4-vinyl pyridine N-oxide) [CNT/PVPNO] 2% cross-linked with divinylbenzene resins was performed by a slightly modification of previously reported procedures [27]. Briefly, CNTs were grinded in agate mortar with the appropriate resin (1:3 w/w CNT/resin) for 20 min at 25 °C. At the end, the material was suspended in EtOAc (5.0 mL) and the support was recovered by centrifugation (12.000 rpm). Next, the grinded supports (5 mg) were suspended in EtOAc (5.0 mL) and treated with MTO (1:2 w/w) under magnetic stirring at 25 °C for 2 h. The novel catalysts [CNT/PVP]/MTO IV and [CNT/PVPNO]/MTO V were recovered by centrifugation (12.000 rpm), washed with a low amount of EtOAc (2.0 mL) and dried. The washing solvent was stored in order to evaluate the LF.

2.3. Catalytic test

2.3.1. Oxidation of thiophene derivatives 1–5. General procedure

Dibenzothiophene (DBT) 1, 4,6-dimethyl-dibenzothiophene (DMDBT) 2, 2-methyl-benzothiophene (2-MeBT) 3, 3-methyl-benzothiophene (3-MeBT) 4, and 3-methyl thiophene 5 (3-MeT), were oxidized as representative aromatic sulfur compounds in fuel oil. Initially, DBT 1 was treated with catalysts I–V and H$_2$O$_2$ in CH$_2$Cl$_2$ or n-octane. Briefly, the appropriate catalyst (3% w/w of MTO with respect to substrate) was added to 1 (0.1 mmol) in CH$_2$Cl$_2$ or n-octane (2.0 mL), followed by treatment with H$_2$O$_2$ (4.0 equivalents, 35% water solution), under magnetic stirring at 60 °C for 24 h. The progress of the oxidation was monitored by GC–MS analysis of periodically withdrawn samples (2.0 μL of sample were taken out the reaction solution). The catalyst was recovered by filtration and MnO$_2$ (1.0 mg) was added under stirring at 25 °C to eliminate the excess of H$_2$O$_2$ (the reaction mixture was found to be unchanged after the MnO$_2$ treatment). The organic solvent was dried on Na$_2$SO$_4$, filtered and evaporated under reduced pressure. Next, the oxidation of compounds 1–5 with catalysts I–V was repeated under similar experimental conditions using n-octane/CH$_3$CN mixture in three different ratio (1:1, 2:1 and 3:1 v/v ratio), to evaluate the optimal amount of the co-solvent. At the end of the oxidation, the catalyst was removed by centrifugation (12.000 rpm), the n-octane and CH$_3$CN phases were separated, dried and analysed by GC–MS in the presence of acetophenone as internal standard. As expected, sulfone derivatives were detected in the polar CH$_3$CN phase. When necessary, crude sulfone derivatives were obtained by distillation

under reduced pressure of the *n*-octane and CH$_3$CN phases, and the recovered organic phases were used for further transformations.

2.3.2. Catalyst recycling and leaching experiments

Recycling experiments with catalyst **V**, as a selected representative sample, were performed for the oxidation of either DBT **1** alone or MF, in the optimal *n*-octane/CH$_3$CN mixture (3:1 v/v) for **1**, or MF/CH$_3$CN (3:1 v/v) for MF. After the first run, the catalyst was recovered by filtration, washed with *n*-hexane and dried under vacuum for 1 h. More runs were performed, working under optimized experimental conditions. To evaluate the presence of a real heterogeneous catalytic activity, the organic layer obtained after any recycle was analyzed by ^{1}H NMR analysis, as previously reported for the determination of the loading factor (LF). The absence of the characteristic ^{1}H NMR Re-Me peak at 2.6 ppm, even after the last recycling run, suggested that MTO was not released in the reaction medium, thus working as purely heterogeneous system. These data were further confirmed by the lack of catalytic activity for the recovered organic solution.

2.3.3. Preparation and oxidation of model fuel (MF) and synthetic diesel fuel (SDF) samples

The model fuel (MF) sample was prepared by adding equimolar amounts (in the range of 0.01–0.03 mmol) of each substrate **1–5** into *n*-octane (from 1.5 to 2.0 mL), in order to obtain a total sulfur concentration of 2.8 mg/mL, which is indicative of a real sample. In a similar way, equimolar amounts (0.02 mmol) of each substrate **1–5** were added to an authentic sample of diesel fuel (SDF, 1.5 mL) to gain a total sulphur concentration of 3.8 mg/mL. The MF and SDF samples were oxidized with the most reactive catalyst **V**, under previously optimized experimental conditions. In particular, MF or SDF samples added with one third of acetonitrile (with respect to their original volume) were treated with catalyst **V** (3% w/w of MTO with respect to total substrate) and H$_2$O$_2$ (4.0 equiv., added in two steps to reduce thermal decomposition; 8.0 equiv. in the case of SDF), under magnetic stirring at 60 °C. The reaction progress was monitored by GC–MS analyses of periodically withdrawn samples (0.1 mL samples were taken out the reaction solution), until the substrate was entirely consumed. At the end of the oxidation, the catalyst was removed by centrifugation (12.000 rpm), the *n*-octane (or diesel fraction) and CH$_3$CN phases were separated, dried and analysed by GC–MS in the presence of acetophenone as internal standard. The sulfone derivatives were detected in the polar CH$_3$CN phase.

3. Results and discussions

3.1. Preparation of catalysts I–V

Three novel types of MTO heterogeneous catalysts were prepared starting from commercially available carbon nanotubes (CNTs). CNTs are excellent supports for immobilization of active organometallic compounds, since they offer a high surface area for loading, as well as biocompatibility and mechanical resistance [28]. Initially, MTO was loaded on CNTs through physical adsorption by noncovalent interactions [29]. In particular, MTO was added to a suspension of CNTs in EtOAc (1:1, 1:2 and 1:5 CNT/MTO w/w ratio) under magnetic stirring at 25 °C for 2 h. CNT/MTO **I** was recovered by centrifugation, washed and used without any further purification (Scheme 1, pathway A). The loading factor (LF) of catalyst **I** (defined as mmol of MTO per gram of support) was measured by ^{1}H NMR titration of the residual MTO in washing solutions, and in alternative, by inductively coupled plasma mass spectrometry (ICP-MS) analysis of the final product. Irrespective to experimental conditions, low values of LF were obtained

(Table 1, entry 1), suggesting the ineffectiveness of the simple physical adsorption of MTO on CNTs. CNTs and poly(4-vinylpyridine) (PVP) undergo metal-induced self-aggregation processes to form tight stable bundles in which metal ions can be trapped by coordination with the pyridinyl moiety [30]. On the basis of these data, we evaluated the possibility to load two preformed MTO adducts, namely poly(4-vinylpyridine)/MTO [PVP·MTO] and poly(4-vinylpyridine)*N*-oxide/MTO [PVPNO·MTO] on CNTs. The adducts were prepared as previously reported by us [16,31], and added to a suspension of CNTs in EtOAc [2:1 w/w, (resin·MTO)/CNT ratio] under magnetic stirring at 25 °C for 2 h, to yield catalysts CNT/[PVP·MTO] **II** and CNT/[PVPNO•MTO] **III** (Scheme 1, pathway B). LFs and immobilization yields of catalysts **II** and **III** were in the range of 0.33–0.36, and 16.6–17.9%, respectively (Table 1, entries 2 and 3).

Finally, we applied the wrapping procedure. The wrapping procedure in solid state [32] is the simplest alternative to physical adsorption for the functionalization of CNTs. For example, the wrapping of PVP on CNTs successfully separates single walled carbon nanotubes from the ropes they formed because of intra-strand van der Walls attractive interactions. Moreover, CNTs wrapped PVP systems show highly modified solubility properties [33]. As a general procedure, PVP (or PVPNO) and CNTs (2:1 w/w ratio) were grinded in an agate mortar for 1 h at 25 °C to afford the desired [CNT/PVP] and [CNT/PVPNO] composite supports [27]. About the efficacy of the deposition, previously reported thermogravimetric analysis (TGA) of [CNT/PVP] showed the presence of c.a. 0.04 mmol of PVP per mg of aggregate [30]. Successively, [CNT/PVP] and [CNT/PVPNO] were dispersed in EtOAc (2.0 mL) and loaded with MTO (composite support:MTO ratio 1:2 w/w) under magnetic stirring for 2 h at 25 °C, to yield [CNT/PVP]/MTO **IV** and [CNT/PVPNO]/MTO **V**, respectively (Scheme 1, pathway C). Catalyst **IV** and **V** showed values of LF and immobilization yield higher than **II** and **III** (Table 1, entries 4–5 versus entries 2–3), confirming the efficacy of the wrapping procedure for the deposition of MTO on CNTs.

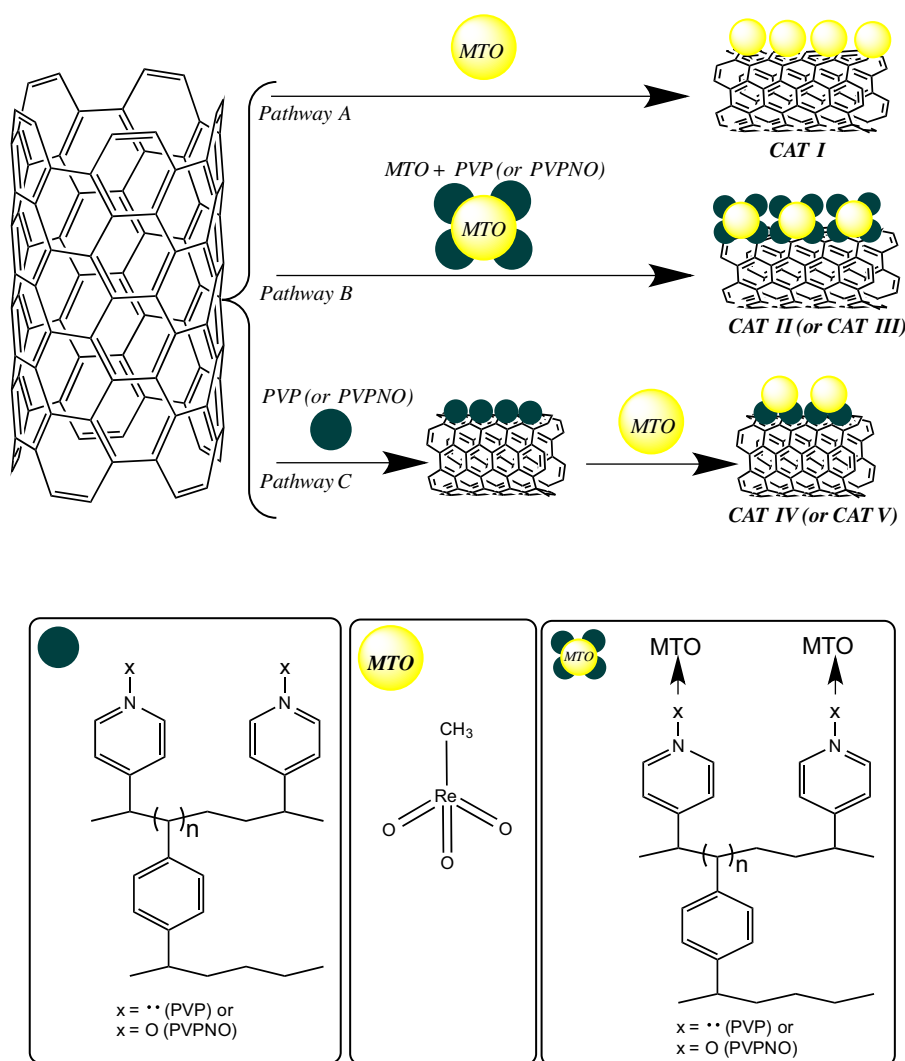### 3.2. Morphological characterization of catalysts II–V

Figs. 1–5 show a set of scanning electron microscopy (SEM) and transmission electron microscopy (TEM) images of catalysts **II–V**. Fig. 1 reports the TEM image of the commercially available CNTs used in the preparation of catalysts **I–V**. CNTs are rigid rods, with a perfectly smooth surface and different diameter depending on the number of the graphitic cylinders involved [34].

SEM and TEM images of catalyst **II** showed a quite different morphology (Fig. 2). The organic resin clearly covers CNTs in the SEM image, yielding objects of fusiform shapes and diameter of average size of the order of 200 nm (Fig. 2, panel A). TEM confirms the coating, the fusiform CNTs black core being homogeneously coated along its extension (Fig. 2, Panel B). At a largest magnification (Fig. 2, panel C), small protrusions emerging from the surface are visible.

The morphology of catalyst **III**, is similar to that of catalyst **II**. Again, CNTs are completely coated by the organic resin (Fig. 3, panel A), that appears as a continuous layer in the TEM image (Fig. 3, panel B).

The wrapping procedure afforded objects with a more organized surface structure. The SEM image of catalyst **IV** shows coated CNTs with small and well defined protrusions of regular shape, arranged on the surface (Fig. 4, panel A). Protrusions are clearly visible as polygonal-like small grumes (Fig. 4, panels A and B). The scaffold was characterized by an average size of the order of 200–300 nm, similar to that of catalyst **II**.

Catalyst **V** showed a behavior similar to **IV**, again characterized by well-defined protrusions on the surface (Fig. 5, panels A and B). The presence of regular aggregates after the wrapping procedure

Scheme 1. Preparation of novel heterogeneous catalysts **I–V**.

Table 1
Composition, loading factor (LF) and immobilization yield (IY) of catalysts **I–V**.

Entry	Sample	Composition	Method[a]	LF[b]	IY[c] (%)
1	Cat **I**	CNT/MTO	i	0.01[d] (n.d.)[e]	0.4[e]
2	Cat **II**	CNT/[PVP•MTO]	ii	0.33[d] (0.31)[e]	16.6[e]
3	Cat **III**	CNT/[PVPNO•MTO]	ii	0.36[d] (0.32)[e]	17.9[e]
4	Cat **IV**	[CNT/PVP]/MTO	iii	0.47[d] (0.42)[e]	24[e]
5	Cat **V**	[CNT/PVPNO]/MTO	iii	1.43[d] (1.40)[e]	71.6[e]

[a] i: by suspension in EtOAc; ii: by mortar grinding [27]; iii: by mortar grinding and suspension in EtOAc.
[b] LF = mmol of catalyst (MTO) per gr of support.
[c] Immobilization yield is defined as supported MTO with respect to total MTO.
[d] Value calculated by ICP-MS analysis.
[e] Value calculated by ^{1}H NMR analysis.

is in accordance with the known supramolecular self-assembling properties of PVP resins, which are able to generate highly organized structures by non-covalent (van der Waals, induced dipoles, etc.) and π-interactions [35a-b].

3.3. XPS analysis

Table 2 reports the XPS binding energies (BEs) of catalysts **II–V**, obtained through the fitting procedure of the N 1 s and Re 4f peaks. The Re 4f region showed two different double peaks, corresponding to $4f_{7/2}$ and $4f_{5/2}$ levels, with a spin orbit splitting of 2.4 eV. The BEs peaks at 46.4, 44.1–44.5 and 44.8–45.0 eV were assigned as Re $4f_{7/2}$ level for Re^{7+}, Re$^{5+/4+}$, and Re^{6+} species, respectively. In addition, the band of the pyridine-*N*-oxide fragment was detected at about 403 eV [35d]. The presence of different oxidation state for rhenium suggests the occurrence of redox processes during the immobilization of MTO on the resins. An analogous behavior was previously observed in the XPS analysis of polyaniline/MTO complexes [35c]. In the case of catalysts **III** and **V,** the higher values of BEs peaks positions of Re 4f level (44.8 and 45.0 eV, respectively, assigned to a Re^{6+} oxidation state) with respect to **II** and **IV**, indicates that the redox process is less relevant for the PVPNO resin. The N 1 s peak
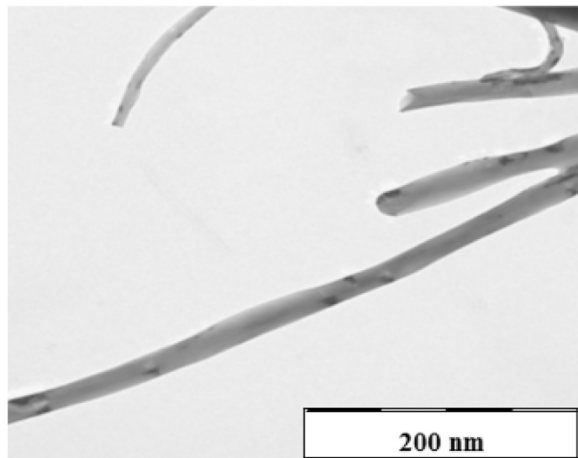
Fig. 1. TEM image of pristine CNTs.
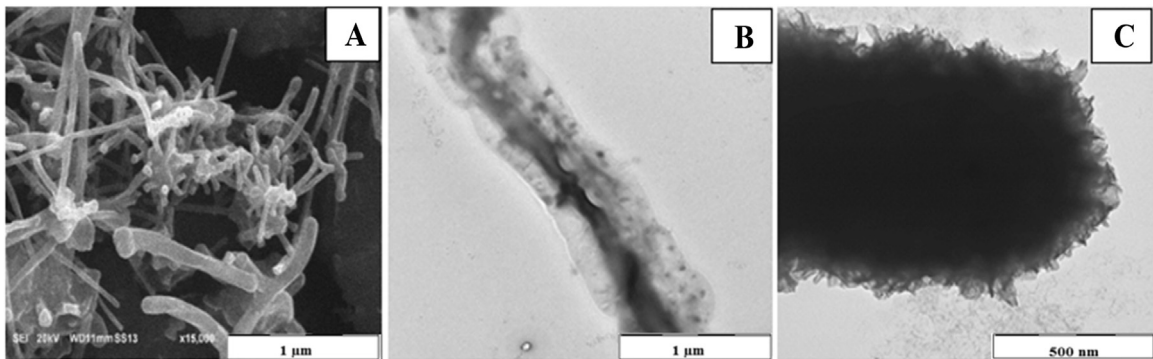

Fig. 2. Panel A: SEM image of catalyst **II**. Panels B and C: TEM images of catalyst **II**.
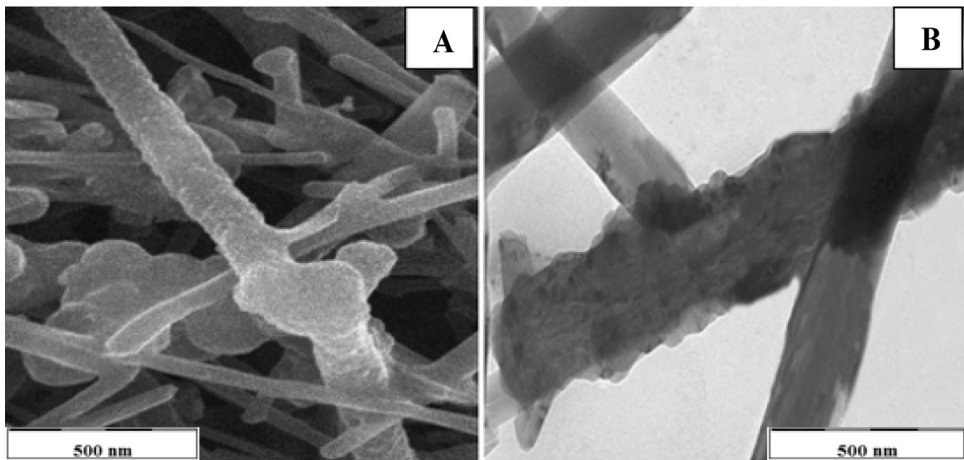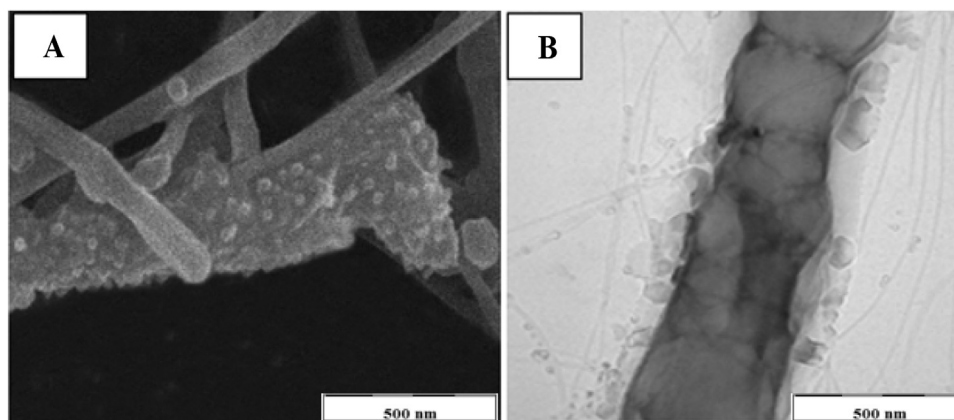

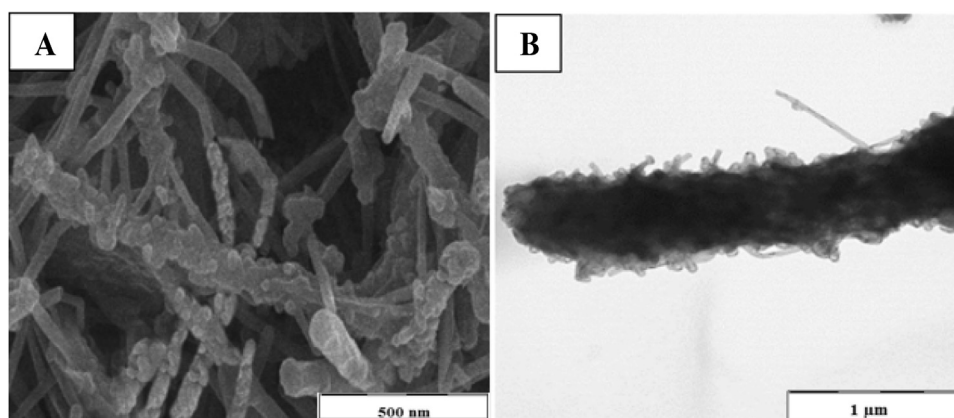**Fig. 3.** SEM image (Panel A) and TEM image (Panel B) of catalyst **III**.

Table 2
Selected Binding Energies (BEs) by XPS analysis on catalysts II–V and relative assignments[a].

Element	II	III	IV	V	Assignments
N $1s$	398.8 401.0 –	399.3 401.1 403.0	399.3 400.9 –	399.2 401.2 402.8	Pyridine[b] Re-pyr interactions Pyridine-N-oxide[b]
Re $4f_{7/2}$	44.1[c] 46.4	44.8[d] 46.4	44.5[c] 46.4	45.0[d] 46.4	Re$^{6+/5+/4+}$ Re^{7+}

[a] BEs measured in eV units.
[b] See Table 5 on reference [35d].
[c] Tentatively assigned to Re$^{5+/4+}$.
[d] Tentatively assigned to Re^{6+}.

Fig. 4. Panel A: SEM image of catalyst **IV** with an organized and regular surface structure. Panel B: TEM image of catalyst **IV** showing protrusions as polygonal-like small grumes.

Fig. 5. Panel A and B: SEM and TEM images of catalyst **V**, respectively.

(at around 401 eV) in catalysts **II–V**, due to a charge transfer from pyridine moiety to rhenium centre, definitively confirms the coordination of rhenium, irrespective to the immobilization procedure.
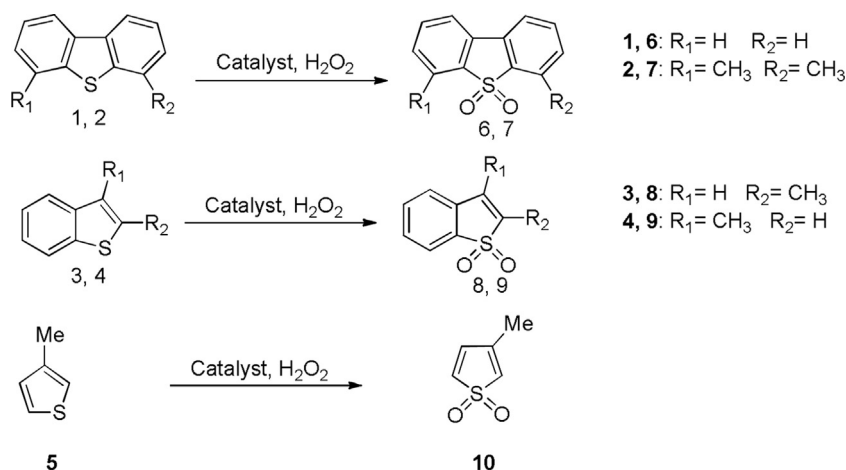
3.4. Oxidation of thiophene, BT and DBT derivatives

In ODS model processes, the oxidation are usually performed in organic solvents with a low value of dielectric constant, since they show a polarity similar to original fuel diesel. With the aim to evaluate the efficacy of catalysts **I–V**, we initially studied the oxidation of DBT **1** in CH_2Cl_2 and *n*-octane, under the experimental conditions previously applied by us with the simple PVP·MTO and PVPNO·MTO adducts [16]. Briefly, the reaction was performed in the presence of the appropriate catalyst (3% w/w of MTO with respect to substrate, based on LF) by addition of a small excess of H_2O_2 (4.0 equiv) in two steps (to reduce thermal decomposition) at 25 °C (CH_2Cl_2) or 60 °C (*n*-octane) [36].

Irrespective to experimental conditions, the sulfone **6** was obtained as the only recovered product, the yield of **6** corresponding to the conversion of substrate (Scheme 2, Table 3, entries 1–12). As expected, catalyst **I** showed a negligible activity, probably due to the low value of LF (Table 3, entries 1 and 6). As reported in Table 3, the oxidation of compound **1** with catalysts **II-V** in CH_2Cl_2 do in quantitative yield and conversion of substrate, to yield the sulfone **6** after only 6 h (Table 3, entries 2–5). A lower reactivity was observed in *n*-octane, in which case higher temperature and longer reaction times were required (Table 3, entries 9–12). The low reactivity of MTO during the oxidation of aromatic sulfur derivatives in *n*-octane was previously reported [16]. Catalysts **II** and **III** showed

a reactivity similar to PVP·MTO and PVPNO•MTO alone, confirming that the adsorption of the MTO adducts on CNTs did not alter their catalytic performance (Table 3, entries 7–8 versus 9–10). On the other hand, catalysts **IV** and **V** were more reactive than catalysts **II** and **III**, catalyst **V** being the most active system (Table 3, entries 11 and 12).

Thus, the properties of the support (wrapped CNTs), and the oxidation state of the resin (that is PVP versus PVPNO) tuned the reactivity of the catalyst, in accordance with the results previously reported for the MTO adducts [31]. This effect may be in part ascribed to the different structure of the active site [16]. Co-solvents with high value of dielectric constant (acetonitrile, DMF and DMSO) have been applied in ODS processes to optimize the sulfur removal, since they can extract the sulfoxide and sulfone derivatives produced during the oxidation [37]. The advantage of the extraction-oxidation process is the high sulfur removal under lower H_2O_2/sulfur ratio, with concomitant improvement of catalyst stability [38]. For this reason, the oxidation of compounds **1** in *n*-octane was repeated with the most active catalyst **V** in the presence of acetonitrile (CH_3CN) in three different ratio values (*n*-octane/CH_3CN, 1:1, 2:1 and 3:1 v/v, respectively) at 60 °C (Table 4, entries 1–3; Scheme 2). CH_3CN really increased the efficiency of the oxidation, leading to formation of sulfone **6** in high yield after 3 h (Table 4, entry 3), the 3:1 *n*-octane/CH_3CN v/v being the optimal mixture (Table 4, entry 1). These experimental conditions were successively applied for the oxidation of compound **1** with catalysts **II–IV** (in this set of experiments catalyst **I** was not analysed, due to its low reactivity). In accordance with data previously reported, catalysts **IV** and **V** were more reactive than **II-III** (Table 4, entries

Scheme 2. Catalytic Oxidation of model aromatic sulfur derivatives **1–5**.

Table 3
Oxidation of DBT **1** to sulfone **6** with catalysts **I–V** in CH_2Cl_2 (25 °C) or n-octane (60 °C)[a].

Entry	Catalyst	Solvent	Time (h)	Yield (%)[b]
1	**I**	CH_2Cl_2	6	<3
2	**II**	CH_2Cl_2	6	>99
3	**III**	CH_2Cl_2	6	>99
4	**IV**	CH_2Cl_2	6	>99
5	**V**	CH_2Cl_2	6	>99
6	**I**	n-octane	24	n.d.
7	**PVP·MTO**[c]	n-octane	24	51
8	**PVPNO·MTO**[c]	n-octane	24	60
9	**II**	n-octane	24	47
10	**III**	n-octane	24	59
11	**IV**	n-octane	24	79
12	**V**	n-octane	24	91

[a] The appropriate catalyst (3% w/w of MTO with respect to substrate) was added to 1 (0.1 mmol) in CH_2Cl_2 or n-octane (2.0 mL), followed by treatment with H_2O_2 (4.0 equivalents, 35% water solution), under magnetic stirring at 25 °C and 60 °C, respectively.
[b] Yields correspond to substrate conversion.
[c] Data from reference [16].

Table 4
Oxidation of thiophene derivatives **1–5** with catalysts **II–V** in n-octane/CH_3CN mixture[a].

Entry	Substrate	Catalyst	Product	Yield (%)
1	1	**V**[b]	6	83
2	1	**V**[c]	6	>90
3	1	**V**	6	>99
4	1	**II**	6	52
5	1	**III**	6	64
6	1	**IV**	6	81
7	1	**PVP•MTO**	6	56
8	1	**PVPNO•MTO**	6	67
9	2	**II**	7	30
10	2	**III**	7	41
11	2	**IV**	7	70
12	2	**V**	7	80
13	3	**II**	8	18
14	3	**III**	8	21
15	3	**IV**	8	69
16	3	**V**	8	78
17	4	**II**	9	16
18	4	**III**	9	21
19	4	**IV**	9	42
20	4	**V**	9	51
21	5	**II**	10	5
22	5	**III**	10	7
23	5	**IV**	10	19
24	5	**V**	10	28

[a] The oxidations were performed with catalysts **II–V** (3% w/w of MTO with respect to substrate) in the presence of n-octane/CH_3CN 3:1 v/v mixture at 60 °C for 3 h.
[b] n-Octane/CH_3CN 1:1 v/v mixture at 60 °C for 3 h.
[c] n-Octane/CH_3CN 2:1 v/v mixture at 60 °C for 3 h.

Table 5
Oxidation of model fuel oil (MF) and synthetic diesel fuel (SDF) samples by either catalyst **V** or PVPNO•MTO.

Entry	Substrates	Solvent	Catalyst	Time (h)	Product (Yield%)
1[a]	**1–4** in MF	n-octane	PVPNO•MTO	2	**6–9** (>99)
2[b]	**1–5**	n-octane/CH$_3$CN	**V**	3	**6** (>99); **7**(80); **8** (78); **9** (51), **10** (28)
3[c]	**1–5** in MF	MF/CH$_3$CN	**V**	2	**6** (>99); **7**(>99); **8** (>99); **9** (>99), **10** (>99)
4[c]	**1–5** in SDF	SDF/CH$_3$CN	**V**	2	**6** (>99); **7**(>99); **8** (>99); **9** (>99), **10** (47)

[a] Experimental conditions as reported in ref. 16: PVPNO•MTO (5% w/w of MTO, LF = 5.0), 4.0 equiv. of H$_2$O$_2$, 1.5 mL of MF having a total S concentration of 2.8 mg/mL, 70 °C.

[b] The oxidations of isolated compounds **1–5** were performed with catalysts **V** (3% w/w of MTO with respect to substrate), 4.0 equiv. of H$_2$O$_2$ in n-octane/CH$_3$CN (3:1 v/v) mixture, at 60 °C.

[c] Catalyst **V** (3% w/w of MTO with respect to substrate), 4.0 equiv. of H$_2$O$_2$ in MF/CH$_3$CN (or 8.0 equiv. of H$_2$O$_2$ for SDF/CH$_3$CN) (3:1 v/v) mixture (2.0 mL), at 60 °C.

3 and 6 versus entries 4 and 5), these latter showing a reactivity similar to PVP•MTO and PVPNO·MTO adducts (Table 4, entries 4–5 versus 7–8). To evaluate the generality of the transformation, the attention was next focused on the oxidation of 4,6-DMDBT **2**, 2-MeBT **3**, 3-MeBT **4**, and 3-MeT **5** (Scheme 2). Irrespective to experimental conditions, sulfones **7–10** were detected as the only recovered products (Table 4, entries 9–24). Again, catalysts **IV** and **V** were the most efficient systems (see for example, Table 4, entries 11–12 versus 9–10, and entries 15–16 versus 13–14). As a general trend, sulfones from dibenzothiophene and monobenzothiophene derivatives (products **6–9**) were obtained in an average yield higher than that from 3-methylthiophene (product **10**), with the following order of reactivity: DBT > 4,6-DMDBT > 2-MeBT ≈ 3-MeBT > 3-MeT. This order of reactivity is in accordance with previously reported data for the oxidation of thiophene derivatives with nanosized catalysts [39], representing the effect of aromatic moieties and electron donating substituents on the electron density of sulfur atom [40,41]. Next, catalyst **V** was applied to a model fuel oil (MF) prepared by addition of equimolar amounts of **1–5** in n-octane, to gain an overall sulfur content of 2.8 mg/mL typical of a real fuel sample [42]. Treatment of the sample mixture MF/CH$_3$CN (3:1 v/v) with catalyst **V** (3% w/w of MTO with respect to total substrate) and H$_2$O$_2$ (4.0 equiv.), at 60 °C yielded the quantitative conversions of **1–5** in 2 h (Table 5, entry 3). The oxidation of compounds **1–5** in MF was more efficient and faster than that of any isolated substrates, suggesting the presence of synergic effects or autocatalysis phenomena (Table 5, entry 3 versus entry 2). Noteworthy, the highly recalcitrant substrate **5** was oxidized in a quantitative manner. In this latter case, the disproportionation reaction between two sulfoxide (or sulfoxide and sulfoxide-like) intermediates might be responsible for the increased yield of sulfones from the most recalcitrant substrates [43]. Previously, we observed a similar behaviour in the oxidation of MF with PVP·MTO and PVPNO·MTO [16]. We can emphasize that catalyst **V** was more reactive than the corresponding PVPNO·MTO system in the oxidation of MF, affording the quantitative conversion of substrates **1–5** with a lower LF value (Table 5, entry 3 versus entry 1). Finally, catalyst **V** efficiently oxidized compounds **1–5** when embedded in a real sample such as the synthetic diesel fuel (SDF) sample (3.8 mg/mL of total sulfur content) (Table 5, entry 4).

It is important to note that catalyst **V** showed a similar performance when applied under the optimal conditions to SDF samples larger than 1000 mL, suggesting the feasibility of this process for a large scale application.

Catalyst **V** was a stable system in the oxidation of substrate **1** in n-octane/CH$_3$CN (3:1 v/v ratio) mixture, as selected representative sample. In particular, it was recovered and recycled ten times, with only a slight decrease of the reactivity after the sixth run, after which it was stabilized at around 60% of the initial value (Table 6).

Interestingly, catalysts **V** showed to be a stable system also in the oxidation of a MF sample (Table 6). Irrespective to the type of substrate, the conversion was high until the fifth run, after which it was stabilized at around 65% of the initial value (only in the case of **5** we observed a slightly lower value stabilized around 40%). These results are in accordance with the previously reported trend of stability in ODS processes of heterogeneous catalysts based on other active species. For example, TiO$_2$ nanoparticles retained the catalytic activity in the oxidation of DBT in MF at least for five runs [44], poly-oxometalates (POMs) nanoparticles for ten runs [45], and titanium Ti-modified SBA-15 (Ti-SBA15) for four runs [46].

Leaching experiments were performed to evaluate the absence of MTO in the homogeneous phase. In particular, the organic layer from any recycle of catalyst **V** was analysed by ^{1}H NMR. The absence of the Re-Me peak (2.6 ppm), even after the sixth recycling run, highlighted that MTO was not released during the reaction. These results were further confirmed by the lack of catalytic activity in the washing solutions [47]. Moreover, the value of the total amount of immobilized rhenium was constant during the recycling runs (ICP-MS analysis). Based on these data, the slight decrease of the reactivity after the sixth run may be probably due to the formation of low reactive rhenium species, as confirmed by XPS analysis.

4. Conclusions

The catalysts **IV** and **V**, produced by wrapping and grinding of the corresponding resin before the loading of MTO, showed higher LF values and reactivity than that obtained by inverting the procedure, suggesting that the interaction of the resin with the CNTs surface affects the coordination of MTO. The stability of PVP•MTO and PVPNO•MTO adducts is due to the formation of octahedral complexes between the rhenium atom and two pyridinyl ligands in the resin, oriented in a vicinal *cis*-position [31]. Probably, the wrapping of PVP and PVPNO on CNTs can account for the emergence of favorable low energy configurations of ligands for the chelation of the active metal. Data confirming the high affinity and selectivity in the interaction between CNTs and PVP resin, to yield very stable and spatially organized supra-molecular structures, have been reported [30]. In the case of catalysts **II** and **III**, the efficacy of the coating on CNTs was irrespective to the nature of the MTO adduct, as suggested by their comparable LF values. Instead, the higher LF value of catalyst **V** with respect to **IV** highlights the major efficacy of PVPNO in the complexation of MTO. These data are in accordance with the anionic properties of PVPNO, as consequence of the high charge separation across the N–O bond [48]. The different behavior of catalysts **IV** and **V** with respect to **II** and **III** was further confirmed by SEM and TEM analyses. Even if the coating was effective in both type of systems, catalysts **IV** and **V** showed more regular and organized surface morphologies. The use of CH$_3$CN as co-solvent improved the efficacy of the oxidation of sulfur derivatives. The electron density effect of aromatic moieties and the presence of electron donating substituents tuned the order of reactivity, dibenzothiophene derivatives being more reactive then benzotiophene and thiophene compounds. Interestingly, catalyst **V** showed a reactivity higher than (or within the same order of magnitude) others nano-sized catalysts, such as phosphotungstic acid supported on magnetic mesoporous silica road particles [49], structurally ordered mesoporous TS-1 (meso/TS-1) [50], and MnO$_2$ nanorods (β-MnO$_2$ and α-MnO$_2$) [51]. With respect to iron oxide

Table 6
Stability of catalyst **V** in the oxidation of DBT **1** and MF.[a]

Substrate		Conversion (%)[b]									
		Run no. 1	Run no. 2	Run no. 3	Run no. 4	Run no. 5	Run no. 6	Run no. 7	Run no. 8	Run no. 9	Run no. 10
DBT (**1**)		>99	95	89	87	81	56	64	61	58	65
MF	DBT (**1**)	>99	>99	>99	90	84	68	71	65	61	64
	DMDBT (**2**)	>99	>99	>99	97	93	73	70	61	72	66
	2-MeBT (**3**)	>99	>99	>99	96	90	64	66	61	59	65
	3-MeBT (**4**)	>99	>99	95	87	89	78	72	69	68	67
	3-MeT (**5**)	>99	88	78	67	57	39	43	40	38	45

[a] After the first reaction, catalyst **V** was recovered by filtration; following runs were performed working under the same experimental conditions.

[b] Yields of corresponding sulfones match with substrates conversion values.

systems immobilized on activated carbon [52], for the oxidation of benzothiophene in the presence of CH_3CN catalyst **V** required a lower amount of H_2O_2 (4.0 equivalents versus 18 equivalents), showing an high selectivity to yield only the sulfone derivative. Catalyst **V** was also efficiently applied to the desulfurization of both model fuel oil (MF) and synthetic diesel fuel (SDF). Since sulfone derivatives produced during the oxidation are not toxic [53] and can be re-used as fine chemicals, the ODS process is particularly useful in the circular economy scenario.

Acknowledgements

Appendix A. Supplementary data

Supplementary data associated with this article can be found, in the online version, at http://dx.doi.org/10.1016/j.apcatb.2016.07.037.

References

[1] (a) A.A. Oliveira, I.F. Teixeira, P. Leandro, E.L. Ribeiro, E. Lorencon, J.D. Ardisson, L. Fernandez-Outon, A.A. Waldemar, F. Macedo, C.C. Moura, Appl. Catal. A 456 (2013) 126–134;
(b) I.F. Teixeira, A.A. Oliveira, T. Christofani, C.C. Moura, J. Mater. Chem. A 1 (2013) 10203–10208.
[2] W.F. De Souza, I. Guimaraes, M.C. Guerreiro, L.C.A. Oliveira, Appl. Catal. A 360 (2009) 205–209.
[3] J. Eßer, P. Wasserscheid, A. Jess, Green Chem. 6 (2004) 316–322.
[4] Z. Vít, D. Gulková, L. Kaluža, J. Kupčík, Appl. Catal. B 179 (2015) 44–53.
[5] M. Farhat Ali, A. Al-Malki, B. El-Ali, G. Martinie, M.N. Siddiqui, Fuel 85 (2006) 1354–1363.
[6] (a) Y. Wang, G. Li, X. Wang, C. Jin, Energy Fuels 21 (2007) 1415–1419;
(b) F. Al-Shahrani, T. Xiao, S.A. Llewellyn, S. Barri, Z. Jiang, H. Shi, G. Martinie, M.L.H. Green, Appl. Catal. B 73 (2007) 311–316.
[7] (a) H. Zhao, G.A. Baker, Front. Chem. Sci. Eng. 9 (2015) 262–279;
(b) W. Zhu, H. Li, X. Jiang, Y. Yan, J. Lu, J. Xia, Energy Fuels 21 (2007) 2514–2516.
[8] (a) J.M. Campos-Martin, M.C. Capel-Sanchez, P. Perez-Presas, J.L.G. Fierro, J. Chem. Technol. Biotechnol. 85 (2010) 879–890;
(b) Z. Ismagilov, S. Yashnik, M. Kerzhentsev, V. Parman, A. Bourane, F.M. Al-Shahrani, A.A. Haji, O.R. Koseoglu, Catal. Rev. Sci. Eng. 53 (2011) 199–255.
[9] A. Shaabani, M. Behnam, A.H. Rezayan, Catal. Commun. 10 (2009) 1074–1078.
[10] G.W. Gokel, H.M. Gerdes, D.M. Dishong, J. Org. Chem. 45 (1980) 3634–3639.
[11] A. Kubota, H. Takeuchi, Org. Process Rev. Dev. 8 (2004) 1076–1078.
[12] L. Cedeño Caero, F. Jorge, A. Navarro, A. Gutiérrez-Alejandre, Catal. Today 116 (2006) 562–568.
[13] N.Y. Chan, T.-Y. Lin, T.F. Yen, Energy Fuels 22 (2008) 3326–3328.
[14] O.S. Nonaka, T. Takashima, W.H. Qian, S. Gakkaisi, J. Jpn. Pet. Inst. 42 (1999) 315–320.
[15] (a) J.M. Campos-Martin, M.C. Capel-Sanchez, J.L.G. Fierro, Green Chem. 6 (2004) 557–562;
(b) J.L. García-Gutiérrez, G.A. Fuentes, M.E. Hernández-Terán, F. Murrieta, J. Navarrete, F. Jiménez-Cruz, Appl. Catal. A 305 (2006) 15–20;
(c) M. Ciclosi, C. Dinoi, L. Gonsalvi, M. Peruzzini, E. Manoury, R. Poli, Organometallics 27 (2008) 2281–2286.
[16] A. Di Giuseppe, M. Crucianelli, F. De Angelis, C. Crestini, R. Saladino, Appl. Catal. B 89 (2009) 239–245.
[17] W.A. Herrmann, R.W. Fischer, W. Scherer, M.U. Rauch, Angew. Chem. Int. Ed. 32 (1993) 1157–1160.
[18] M. Crucianelli, R. Saladino, F. De Angelis, ChemSusChem 3 (2010) 524–540.
[19] R. Saladino, G. Botta, M. Crucianelli, Applying Nanotechnology to the Desulfurization Process in Petroleum Engineering, in: T.A. Saleh (Ed.), IGI Global, USA, 2016, pp. 180–215.
[20] Y. Zhai, Z. Zhu, S. Dong, ChemCatChem 7 (2015) 2806–2815.
[21] D. Tasis, N. Tagmatarchis, A. Bianco, M. Prato, Chem. Rev. 106 (2006) 1105–1136.
[22] (a) M.L. Chen, F.J. Zhang, W.C. Oh, New Carbon Mater. 24 (2009) 159–166;
(b) K. Woan, G. Pyrgiotakis, W. Sigmund, Adv. Mater. 21 (2009) 2233–2239;
(c) X. Gui, J. Wei, K. Wang, A. Cao, H. Zhu, Y. Jia, Q. Shu, D. Wu, Adv. Mater. 22 (2010) 617–621.
[23] (a) Catalysts for fine chemical synthesis, in: I.V. Kozhevnikov (Ed.), Catalysis by Polyoxometalates, vol. 2, John Wiley & Sons, Chichester, 2002;
(b) R. Wang, F. Yu, G. Zhang, H. Zhao, Catal. Today 150 (2010) 37–41.
[24] N.M. Meman, M. Pourkhalil, A. Rashidi, B. Zarenezhad, J. Ind. Eng. Chem. 20 (2014) 4054–4058.
[25] N.M. Meman, B. Zarenezhad, A. Rashidi, Z. Hajjar, E. Esmaeili, J. Ind. Eng. Chem. 22 (2015) 179–184.
[26] (a) D. Piccinino, M. Delfino, G. Botta, M. Crucianelli, V. Grossi, M. Passacantando, R. Antiochia, G. Favero, R. Saladino, Appl. Catal. A 499 (2015) 77–88;
(b) F. Subrizi, M. Crucianelli, V. Grossi, M. Passacantando, L. Pesci, R. Saladino, ACS Catal. 4 (2014) 810–822.
[27] H. Jing, W. Zhongguang, Z. Jian, Z. Jin, L. Ruying, N. Hengyong, S. Xueliang, Colloid Polym. Sci. 289 (2011) 783–789.
[28] G. Zhan, H.C. Zeng, Chem. Mater. 27 (2015) 726–734.
[29] U. Hanefeld, L. Gardossi, E. Magner, Chem. Soc. Rev. 38 (2009) 453–468.
[30] L. Maggini, J.-M. Raquez, R. Marega, J.J. Ahrens, F. Pineux, F. Meyer, P. Dubois, D. Bonifazi, ChemSusChem 6 (2013) 367–377.
[31] R. Saladino, A.R. Pelliccia, V. Neri, R. Caminiti, C. Sadun J. Org. Chem. 67 (2002) 1323–1332.
[32] (a) M.J. O'Connell, P. Boul, L.M. Ericson, C. Huffman, Y. Wang, E. Haroz, C. Kuper, J. Tour, K.D. Ausman, R.E. Smalley, Chem. Phys. Lett. 342 (2001) 265–271;
(b) A. Star, J.F. Stoddart, Macromolecules 35 (2002) 7516–7520.
[33] J. Hua, Z. Wang, J. Zhao, L. Xu, J.I. Zhang, R. Li, X. Sun, J. Macromol. Sci. B 50 (2011) 679–687.
[34] C.N.R. Rao, A. Govindaraj, Nanosci. Nanotechnol. 18 (2011).
[35] (a) L. Li, X. Ou, S. Sims, W. Li, L. Wu, RCS Adv. 4 (2014) 56998–57008;
(b) M. Wang, M. Jiang, F. Ning, D. Chen, S. Liu, H. Duan, Macromolecules 35 (2002) 5980–5989;
(c) B.M. Choudary, M. Roy, S. Roy, M.L. Kantam, B. Sreedhar, K. Vijay Kumar, Adv. Synth. Catal. 348 (2006) 1734–1742;
(d) Y. Yan, J. Miao, Z. Yang, F.-X. Xiao, H.B. Yang, B. Liu, Y. Yang, Chem. Soc. Rev. 44 (2015) 3295–3346.
[36] L. Cedeño-Caero, H. Gomez-Bernal, A. Fraustro-Cuevas, H.D. Guerra-Gomez, R. Cuevas-Garcia, Catal. Today 133–135 (2008) 244–254.
[37] C. Patrut, C.S. Bildea, A.A. Kiss, Chem. Eng. Process. 81 (2014) 1–12.
[38] T. Yajie, Y. Yue, Z. Yanhui, Y. Lijun, L. Shuxiang, Energy Fuels 29 (2015) 618–625.
[39] M. Sharifzadeh Baei, M.A. Rezvani, Asian J. Chem. 23 (2011) 5381–5389.
[40] (a) T. Napanang, T. Sooknoi, Catal. Commun. 11 (2009) 1–6;
(b) M. Seredych, T.J. Bandosz, Fuel 108 (2013) 846–849.
[41] K.N. Brown, J.H. Espenson, Inorg. Chem. 35 (1996) 7211–7216.
[42] X. Ma, A. Zhou, C. Song, Catal. Today 123 (2007) 276–284.
[43] H.R. Davis, D.P. Sorensen, US patent 2870215A in Disproportionation of organic sulfoxides. Application February 21, (1956) Serial No. 566,762.
[44] X. Wang, F. Li, J. Liu, C. Kou, Y. Zhao, Y. Hao, D. Zhao, Energy Fuels 26 (2012) 6777–6782.
[45] Y. Chen, S. Zhao, Y.F. Song, Appl. Catal. A: Gen. 466 (2013) 307–314.
[46] E. Lorençon, D.C.B. Alves, K. Krambrock, E.S. Ávila, R.R. Resende, A.S. Ferlauto, R.M. Lago, Fuel 132 (2014) 53–61.
[47] J.A. Moulijn, A.E. van Diepen, F. Kapteijn, Appl. Catal. A 212 (2001) 3–16.
[48] C.M. Lee, E.M. Pearce, T.K. Kwei, Polymer 37 (1996) 4283–4288.

[49] Y. Chen, F. Zhang, Z.X. Fang, W. Zhen, R. Wang, J. Ma, Catal. Commun. 38 (2013) 54–58.

[50] Y. Fang, H. Hu, Catal. Commun. 8 (2007) 817–820.

[51] J.T. Sampanthar, J. Dou, G.G. Joo, E. Widjaja, L.Q.H. Eunice, Nanotechnology 18 (2007) 025601.

[52] G.-J. Wang, J.-K. Zhang, Y. Liu, Korean J. Chem. Eng. 30 (2013) 1559–1565.

[53] P.D. Mosier, P.C. Jurs, L.L. Custer, S.K. Durham, G.M. Pearl, Chem. Res. Toxicol. 16 (2003) 721–732.